

## LIST OF ABBREVIATIONS

- 1TCM – one-tissue compartment model
- 2TCM – two-tissue compartment model
- $BP_{ND}$  – Binding Potential Non-Displaceable (equilibrium concentration ratio of specifically bound radioligand to non-displaceable radioligand in tissue)<sup>1</sup>
- DMF – N,N'-dimethylformamide
- DMSO – dimethylsulphoxide
- GPCR – G-protein coupled receptor
- GTP – guanosine triphosphate
- HPLC – high-pressure liquid chromatography
- HRMS – high-resolution mass-spectrometry
- MOMCl – methoxymethyl chloride
- PET – positron emission tomography
- ROI – region of interest
- SRTM – simplified reference-tissue model
- SUV – standardized uptake value (regional uptake relative to mean uptake across the body)
- TAC – time-activity curve
- THF – tetrahydrofuran
- TLC – thin-layer chromatography
- TsCl – p-toluenesulfonyl chloride
- UPLC – ultra-productive liquid chromatography
- $V_T$  – total distribution volume of a radioligand in the tissue (i.e. the sum of distribution volumes of free, non-specifically and specifically bound radioligand)

## CHEMISTRY

### Materials and methods

Reagents, chemicals, materials and solvents were obtained from commercial sources, and were used as received: Biosolve, Merck for solvents, Cambridge Isotope Laboratories for deuterated solvents, and Aldrich, Acros, ABCR, Merck and Fluka for chemicals, materials and reagents. All solvents were of AR quality.

$^1\text{H}$ -NMR and  $^{13}\text{C}$ -NMR spectra were recorded on Varian MR (300 or 400 MHz for  $^1\text{H}$ -NMR, 100 MHz for  $^{13}\text{C}$ -NMR) spectrometers at ambient temperature. Chemical shifts are reported in ppm, applying deuterated chloroform ( $\text{CDCl}_3$ ) or other deuterated solvents as internal reference. Abbreviations used for splitting patterns are s = singlet, t = triplet, q = quartet, m = multiplet, dd = double doublet.

LC-PDA/MS analyses were performed on a Shimadzu LC-10 AD VP series LC coupled to a photo diode array (PDA) detector (Finnigan Surveyor PDA Plus detector, Thermo Electron corporation) and an ion-trap detector (LCQ Fleet, Thermo Scientific). Analyses were executed at 298 K using an Alltech Alltima HP C18  $3\mu$  column using an injection volume of 1-4  $\mu\text{L}$ , a flow rate of 0.2 mL min $^{-1}$  and typically a MeCN in  $\text{H}_2\text{O}$  gradient (from 5% to 100% MeCN, where both MeCN and  $\text{H}_2\text{O}$  contain 0.1% formic acid).

Elemental analyses and UPLC-HRMS analyses were performed on **AMC20** in its isolated oxalate form. Elemental analyses were done to assess the number of oxalate groups attached to **AMC20** and were performed on a Perkin Elmer Series II CHNS/O Analyser 2400. UPLC-HRMS was used to determine the purity and the exact molecular weight of **AMC20**. UPLC was performed on a Waters Acquity UPLC equipped with a sample manager (an autosampler) and a binary solvent manager. An Acquity UPLC BEH C18 1.7 micrometer column was used applying  $\text{H}_2\text{O}$  and MeCN, both containing 0.1% formic acid, as the two eluents and applying an 8 minute gradient program where

the content of MeCN was increased from 5 to 60% in 5 minutes time. A sample solution (10% MeCN in H<sub>2</sub>O with 0.1% formic acid) with a concentration of ca. 0.1 mg/mL was prepared and an injection volume of 0.1 microliter was used. For HRMS detection, a Xevo G2 Qtof detector using Zspray lockspray ionisation was applied.

Analytical thin layer chromatography (TLC) was performed on Kieselgel F-254 precoated silica plates. Normal phase column chromatography was carried out on flash silica gel (40-63 µm mesh) or regular silica gel (60-200 µm), both acquired from Screening Devices B.V., or on standardized aluminium oxide 90 from Merck.

### **Synthesis of AMC20 reference and precursors**

The synthetic routes to the <sup>19</sup>F-AMC20 and the <sup>18</sup>F-AMC20 precursor amine **5** are outlined in Supplemental Figure 1. The synthesis of all AMC derivatives shown in this figure has been already described in detail elsewhere<sup>2</sup>, except the preparation of AMC20 itself and of its precursor **4**, which is described here. Briefly, all compounds were prepared starting from 2,4-dihydroxyacetophenone (**1**) that was converted in two steps<sup>3,4</sup> and a third lipase kinetic resolution step<sup>5</sup> to the key AMC-intermediate (*R*)-ethyl 7-hydroxychroman-2-carboxylate (**2**). The 7-hydroxyl group of the chromane moiety of **2** was protected by the methoxymethyl (MOM) group, the ethyl ester group was reduced to the primary alcohol, and this alcohol was tosylated to arrive at molecule **3**. ‘Cold’ AMC20 was obtained by coupling of **3** with *p*-fluorobenzylamine to give molecule **4** and then removing the MOM protecting group. Secondary amine AMC20 was converted to its oxalate salt, and this salt was used in the assays that are described in this manuscript. Finally, tosylate **3** was used in a standard two-step Gabriel synthesis to prepare primary amine **5**.

### **(R) N-[7-(Methoxymethoxy)chroman-2-yl]methyl 4-fluorobenzyl amine (4)**

Tosylate **3** (250 mg, 0.66 mmol), commercially available 4-fluorobenzylamine (124 mg, 0.99 mmol, 1.5 moleqs) and DIPEA (341 mg, 2.64 mmol, 4 moleqs) were dissolved in DMSO (5 mL). The reaction mixture was stirred for 24 hours at 85 °C, and was then poured into ice water. The aqueous layer was extracted with ethyl acetate to yield crude product that was purified by alumina column chromatography (2% MeOH/CHCl<sub>3</sub>). Yield: 124 mg (57%).

<sup>1</sup>H NMR (CDCl<sub>3</sub>): δ = 7.30 (m, 2H), 7.00 (m, 2H), 6.93 (m, 1H), 6.53 (multiple signals, 2H), 5.08 (s, 2H), 4.15 (m, 1H), 3.85 (s, 2H), 3.45 (s, 3H), 2.9-2.6 (multiple signals, 4H), 1.93 (m, 1H), 1.8 (multiple signals, 2H). LC-MS: *m/z* = 332.4 [M+H]<sup>+</sup>, (calcd 331.39 for C<sub>19</sub>H<sub>22</sub>NO<sub>3</sub>F).

#### **(R)-2-[(4-Fluorobenzylamino)methyl]chroman-7-ol (AMC20)**

The MOM-protected secondary amine **4** (125 mg, 0.378 mmol) was dissolved in a 4M HCl solution in dioxane (2 mL) and isopropanol (2 mL). The reaction mixture was stirred for about 3 hours at rt, while a N<sub>2</sub> flow was maintained over the reaction mixture. From time to time, N<sub>2</sub> was bubbled through the solution in order to remove volatile reaction products from the mixture. The reaction mixture may turn hazy due to precipitation of the ammonium salt. After completion of the reaction (the reaction was monitored by LC-MS), the mixture was added to water and the pH was brought to slightly basic by addition of a NaOH-solution. The free amine oil product was isolated from the water layer by several extractions using CHCl<sub>3</sub> or CH<sub>2</sub>Cl<sub>2</sub> with some added THF, followed by drying of the collected organic layers with Na<sub>2</sub>SO<sub>4</sub> and evaporation of the solvent.

Yield 63 mg (58%).

<sup>1</sup>H NMR (CDCl<sub>3</sub>): δ = 7.35 (m, 2H), 7.0 (m, 2H), 6.77 (m, 1H), 6.30 (multiple signals, 2H), 4.05 (m, 1H), 3.90 (d, 1H), 3.85 (d, 1H), 2.85-2.75 (multiple signals, 2H), 2.7-2.5 (multiple signals, 2H), 1.8 (m, 1H), 1.7 (m, 1H). <sup>13</sup>C NMR (CDCl<sub>3</sub>): δ = 163.5, 161.0, 156.1, 154.4, 133.5, 130.5, 130.4, 130.1, 115.6, 115.4, 112.6, 109.2, 103.2, 74.1, 53.4, 53.2, 26.2, 23.6. LC-MS: *m/z* = 288.4 [M+H]<sup>+</sup>, (calcd 287.33 for C<sub>17</sub>H<sub>18</sub>NO<sub>2</sub>F).

**Preparation of the oxalate salt of AMC20:** the free amine of **AMC20** (63 mg, 0.219 mmol) was dissolved in THF (3 mL) and oxalic acid dihydrate (61 mg, 0.484 mmol, 2.2 moleqs) in THF (1 mL) was added. The reaction mixture turned hazy due to precipitation of the oxalate ammonium salt. After about 3-5 hours of stirring the reaction mixture was centrifuged and the solvent was pipetted or decanted off. The residue was stirred in a fresh 1:1 mixture of diethyl ether and THF, and was centrifuged again. The solvent was removed and the precipitate was dried to yield a white solid residue (41 mg, 50%).

$^1\text{H}$  NMR (DMSO- $d_6$ ):  $\delta$  = 6.0-3.5 (broad signal acidic protons), 7.55 (m, 2H), 7.25 (m, 2H), 6.8 (m, 1H), 6.3 (m, 1H), 6.25 (s, 1H), 4.25 (m, 1H), 4.2 (m, 1H), 3.2-3.0 (m, 2H), 2.75-2.6 (multiple signals, 2H), 2.0 (m, 1H), 1.65 (m, 1H).  $^{13}\text{C}$  NMR (DMSO- $d_6$ ):  $\delta$  = 164.0, 163.4, 161.3, 156.5, 153.9, 132.4, 132.3, 129.9, 128.9, 115.6, 115.4, 111.9, 108.5, 102.9, 71.6, 49.9 (2Cs), 24.7, 22.8. LC-MS:  $m/z$  = 288.4 [M+H] $^+$ , (calcd 287.33 for  $\text{C}_{17}\text{H}_{18}\text{NO}_2\text{F}$ ). HRMS [M+H] $^+$ : Calcd 288.1400, Found 288.1403 (1.0 ppm). Anal.  $\text{C}_{17}\text{H}_{18}\text{NO}_3\text{F} + \text{C}_2\text{H}_2\text{O}_4$  (FW=377.37).

## **RADIOCHEMISTRY**

### **Materials**

$^{18}\text{F}$ -fluoride was produced in the Scanditronix MC-17F cyclotron (GE Healthcare) and delivered from the target into the hotcell with helium overpressure. Synthetic procedures were performed manually. Radiochemical conversions and purities were determined by radio-HPLC using beta-sensitive detectors and dose-calibrators (Veenstra Instruments) and by radio-TLC using Cyclone phosphor storage screens (multisensitive, Packard) and OptiQuant software.

### **$^{18}\text{F}$ -fluoride production and drying**

$^{18}\text{F}$ -fluoride in enriched  $^{18}\text{O}$ -water was adsorbed on an anion-exchange column (QMA) (pre-activated with  $\text{NaHCO}_3$  solution) and then eluted from it into the drying vial with 1-1.5 ml of  $\text{K}_2\text{CO}_3$ -Kryptofix solution in 9:1 v/v mixture of acetonitrile and water, respectively. After the elution of QMA, acetonitrile and water were evaporated at  $130^\circ\text{C}$  under nitrogen flow. For further water removal, 1 ml anhydrous acetonitrile was added into the reaction vial and evaporated. The operation was repeated three times. In total,  $^{18}\text{F}$ -fluoride drying process took about 15 min.

### **Preparation of $^{18}\text{F}$ -AMC20**

Trimethylammonium benzaldehyde triflate (2 mg) in 1 mL anhydrous DMSO were added into the vial with dried  $^{18}\text{F}$ -fluoride (prepared as described above) complexed with  $\text{K}_2\text{CO}_3$  (1.5-2.2 mg) and 5-7.5 mg/ml Kryptofix. The vial was sealed and the reaction was carried out for 2.5 min at  $130^\circ\text{C}$  followed by cooling for 5 min. Then 1 mL of water was added to the cooled reaction mixture.  $^{18}\text{F}$ -FBA was purified by reverse-phase HPLC using Platinum C18 EPS 5u 250x10 mm column eluted

with acetonitrile/10 mM H<sub>3</sub>PO<sub>4</sub> (40/60 v/v) at 4 ml/min (retention time 9.7 min, k' = 3.0). Collected radioactive fraction was diluted 2-3 fold with water and 4-<sup>18</sup>F-fluorobenzaldehyde was adsorbed on Oasis HLB SPE cartridge. The cartridge was rinsed with 5 mL of pure water and dried for 5 min in strong nitrogen flow. Afterwards 4-<sup>18</sup>F-fluorobenzaldehyde was eluted from the cartridge with 0.9 mL methanol (cartridge was eluted in reverse position; about one third of ethanol got absorbed by the resin) into a v-vial containing primary amine **5** (0.6 mg) and NaBH<sub>3</sub>CN (2 mg) in 100 µl methanol. 5 µl glacial acetic acid was added into the vial, the vial was sealed and reductive amination was conducted for 10 min at 120 °C. The vial was allowed to cool down for 2-3 min, then 1 mL 0.4N HCl was added into it to allow for deprotection of the MOM-group that lasted 10 min at 120 °C. <sup>18</sup>F-**AMC20** was purified by reverse-phase HPLC using Platinum C18 EPS 5u 250x10 mm column eluted with acetonitrile/10 mM H<sub>3</sub>PO<sub>4</sub> (50/50 v/v) at 5 mL/min (retention time 10.1 min, k' = 4.1).

The collected HPLC fraction was diluted with 10 volumes of water and <sup>18</sup>F-**AMC20** was adsorbed on an Oasis HLB SPE cartridge. The cartridge was rinsed with 5 mL pure water and <sup>18</sup>F-**AMC20** was then eluted with 1-2 mL absolute ethanol (typically giving a 50% recovery). After partial or complete evaporation of ethanol in nitrogen flow (with or without application of vacuum) the tracer was formulated in physiological saline (ethanol content in the formulated tracer was kept below 10%). The identity of <sup>18</sup>F-**AMC20** was confirmed and the radiochemical purity was assessed by reverse-phase HPLC and radio-TLC, respectively. Reverse-phase HPLC was carried out on Platinum EPS 5u 250x4.6 column eluted with acetonitrile/water/formic acid (60/40/0.1 v/v) at 2 mL/min (retention time 14.7 min, k' = 13.6). Radio-TLC was carried out on silica plates eluted with ethylacetate/methanol/triethylamine (100/5/1, R<sub>f</sub> = 0.61) and hexane/ethylacetate/triethylamine (50/50/1, R<sub>f</sub> = 0.28).

## **PHARMACOLOGY**

### **Arrestin recruitment assay**

Agonism of AMC20 at D<sub>2</sub> receptors was determined with the PathHunter™ eXpress DRD2L CHO-K1 β-Arrestin GPCR Assay (catalog number 93-0446CP2M) from DiscoverX (Fremont, CA), used according to the supplied protocol. At first 8000 cells/well were seeded in a 96-well plate and incubated 48 hours at 5% CO<sub>2</sub> and 37°C. Then dilutions of AMC20 were added and the plates were incubated for 90 minutes at 5% CO<sub>2</sub> and 37 °C. After that the detection mixture was prepared and added to the assay. Subsequently the plates were incubated for 60 minutes at room temperature after which chemiluminescence was measured on a multiplate reader (Victor 2, Wallac, Perkin Elmer).

### **In vitro autoradiography assay**

Frozen brains of young (10-12 weeks of age; 300-350 g body-weight) male Sprague-Dawley rats (Harlan, Netherlands) were cut into two halves along the sagittal symmetry plane. Each half was mounted, lateral side up, on a paper slide pre-treated by Tissue-Tek fixing cocktail (Sakura, the Netherlands) and fixed by placing it onto a Petri dish floating on liquid nitrogen. After fixing, brains were cut at -12°C into sagittal slices 20 μm thick using a Leica microtome, and the slices were thaw-mounted on Superfrost (70x22 mm, Fischer) adhesive slides. Only slices containing both striatal and cerebellar regions (representing non-specific binding) were used. Slides were organized in pairs and in each pair new slices were mounted alternately on the first or the second slide of the pair, so that slices in corresponding positions on the two slides forming a pair would represent adjacent tissue layers. The slices were allowed to dry, then put into storage boxes with desiccator (silicagel) bags and kept at -80°C until they were used (no longer than 1 week).



On the day of the experiment the slides with mounted slices were taken out of storage and allowed to come to room temperature for 5-10 minutes. After that, incubation buffer (50 mM Tris-HCl, 5 mM KCl, 2 mM CaCl<sub>2</sub>, 2 mM MgCl<sub>2</sub>, 120 mM NaCl, pH 7.4 25°C) was applied to the slides using an automatic pipette (1-1.2 ml/slide) and the slides were pre-incubated for 15 min at room temperature. The pre-incubation buffer was then removed and the slides were placed into staining jars containing incubation buffer and radioligand (<sup>18</sup>F-**AMC20**) with or without 10 μM raclopride (D<sub>2/3</sub>-antagonist) or 100 μM guanosine-5'-triphosphate sodium salt (GTP, stimulator of G-protein uncoupling from the receptors). The slides were incubated for 35 min at 37°C, then washed once with ice-cold incubated buffer (3.5 min) and dipped for 30 s into ice-cold sterile water to remove buffer salts.

After drying the slides in a stream of room-temperature air, they were exposed on phosphor storage screens for 6-10 hours. Afterwards the storage screens were read by Cyclone Storage Phosphor System (Packard Instruments Co). Quantification of plate readings was done with Optiquant software (version 3.00, Packard Instruments Co), drawing regions of interest manually on the striatum and cerebellum.

## **ANIMAL TISSUES WORKUP**

### **Measuring the whole blood time-activity curve and metabolite-corrected plasma input curve**

25 µl aliquots of whole blood were withdrawn from each arterial blood sample taken from each rat. The rest was centrifuged at 3500 g for 5 min, and 25 µl supernatant (plasma) aliquots were withdrawn and deproteinated with 75 µl of ice-cold acetonitrile. From the resulting 100 µl, 2-8 µl portions (i.e. 2-8% of volume) were taken for thin layer chromatography analysis (radio-TLC), to assess radiometabolite content. Radio-TLC was performed on silica plates. Samples of the formulated tracers (diluted) were run along with deproteinated plasma samples to confirm the identity of the parent compound in plasma. Eluent system was ethylacetate/methanol/triethylamine 100/5/1, recorded  $R_f$  of  $^{18}\text{F}$ -**AMC20** was 0.65.

The radioactivity of the plasma and whole blood samples was measured using a well-type gamma-counter (LKB-1282-Compugamma, LKB Wallac).

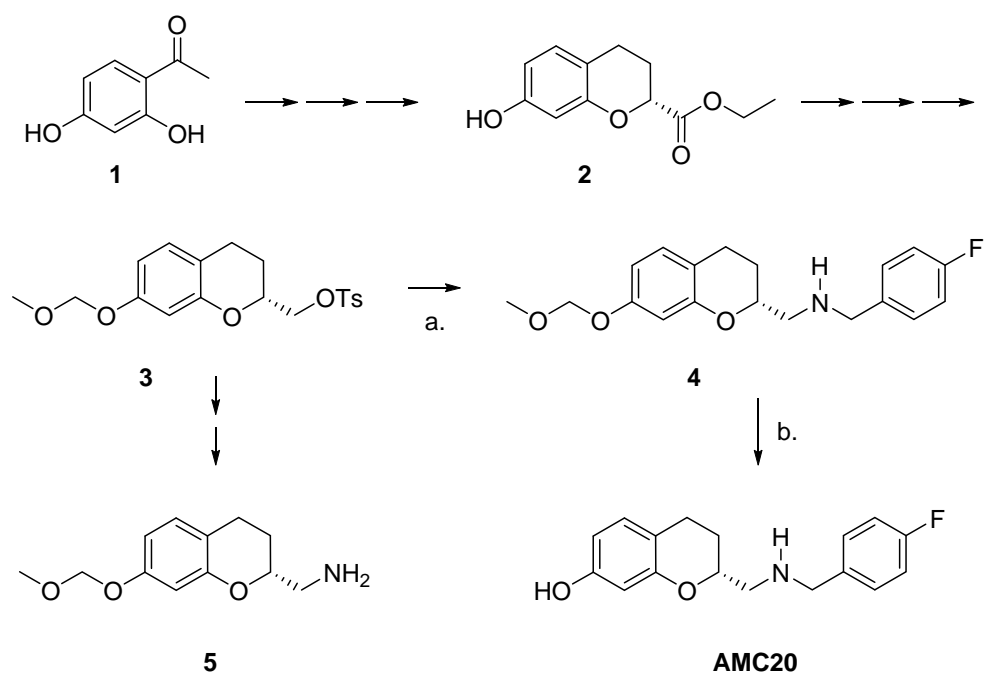
### **Ex vivo autoradiography**

The selected half of the brain (rostral or randomly taken left/right) was quickly frozen over liquid nitrogen and prepared for cutting on the microtome in the same manner as brains used for in vitro autoradiography (see above). 40 µm thick slices were cut, mounted on Superfrost glass slides, permitted to dry and then directly applied to the phosphor storage screens.

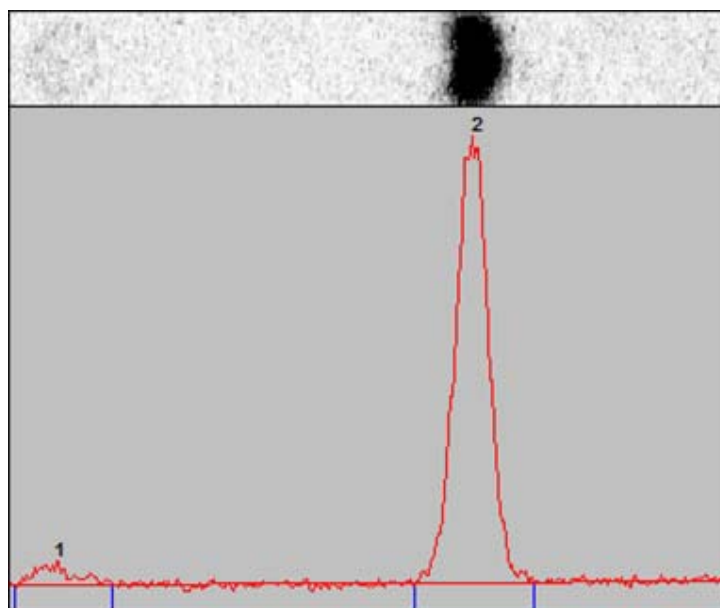
### **Brain radiometabolite analysis**

The half of the brain not selected for ex vivo autoradiography was homogenized in 3 ml ice-cold acetonitrile using Heidolph IDAX600 homogenizer at maximum speed. Homogenate was

centrifuged at 3500 g for 5 min and the supernatant (containing >95% total radioactivity) was analyzed by radio-TLC in the same way as described above for the plasma.

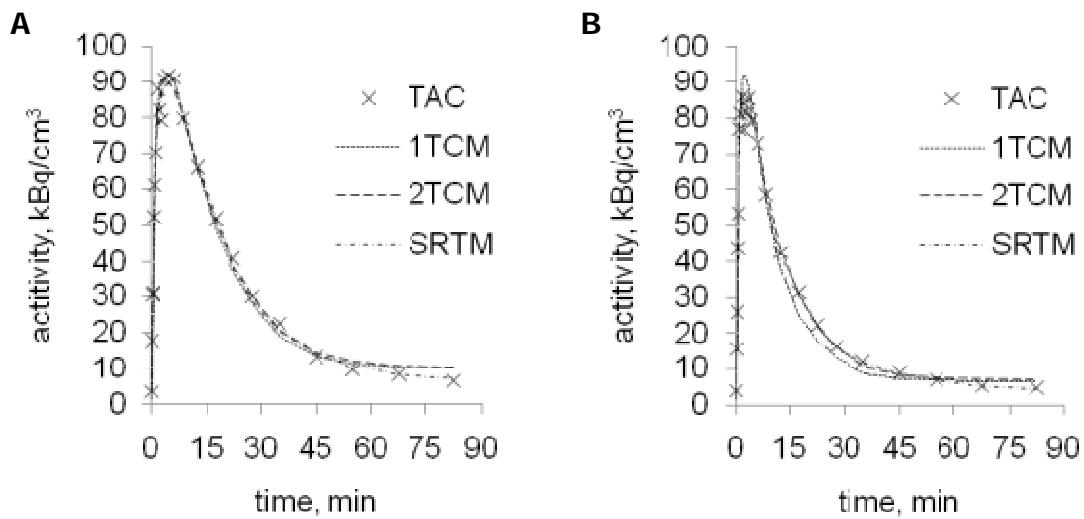


**Supplemental Figure 1.** The scheme of synthesis of unlabeled **AMC20** and of primary amine **5**, the precursor to  $^{18}\text{F}$ -**AMC20**. Reagents and solvents: (a) *p*-fluorobenzylamine, DIPEA, DMSO; (b) 4M HCl, dioxane/isopropanol.



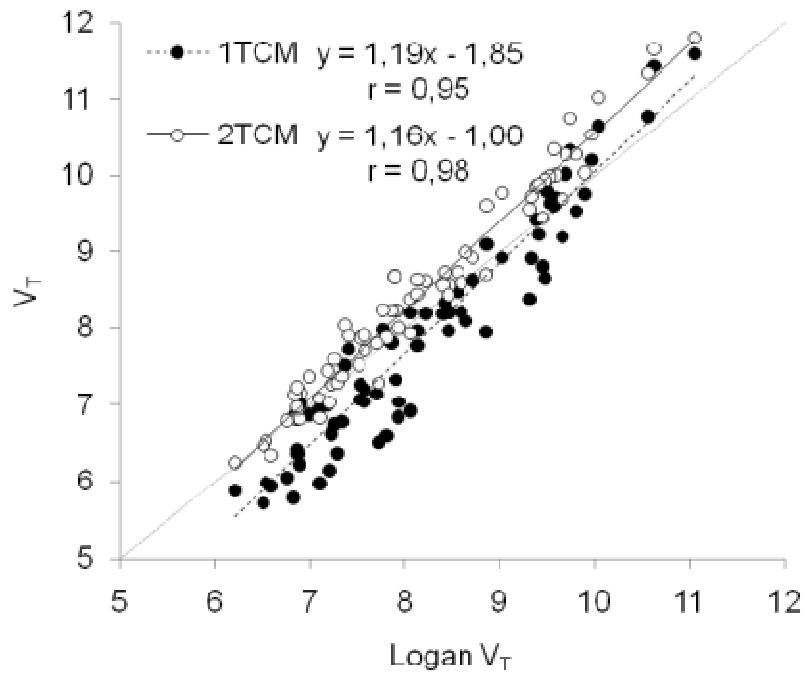
**Supplemental Figure 2.** Radio-TLC analysis of brain tissue radiometabolites of  $^{18}\text{F}$ -AMC20.

A representative TLC lane is shown, as an actual image (top) and as a profile graph of total exposure (bottom). Solvent system is ethylacetate/methanol/triethylamine (100/5/1). Solvent front movement is left-to-right. Peak 1 represents radiometabolites of  $^{18}\text{F}$ -AMC20, peak 2 represents intact  $^{18}\text{F}$ -AMC20.



**Supplemental Figure 3.** Representative striatal (A) and cerebellar (B) TACs of  $^{18}\text{F}$ -AMC20 (in a control rat) and the corresponding fits with 1TCM, 2TCM and SRTM models.

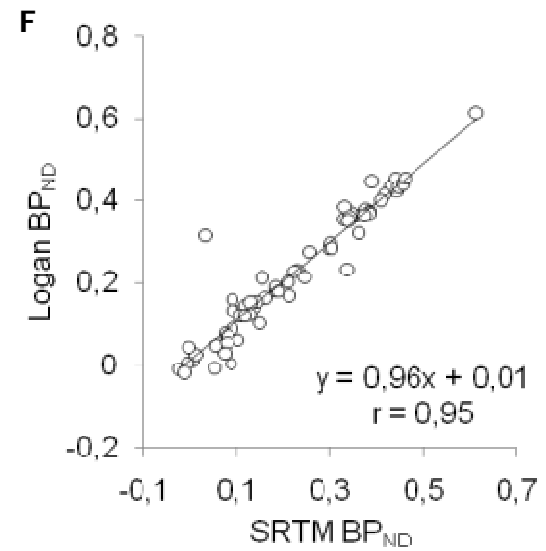
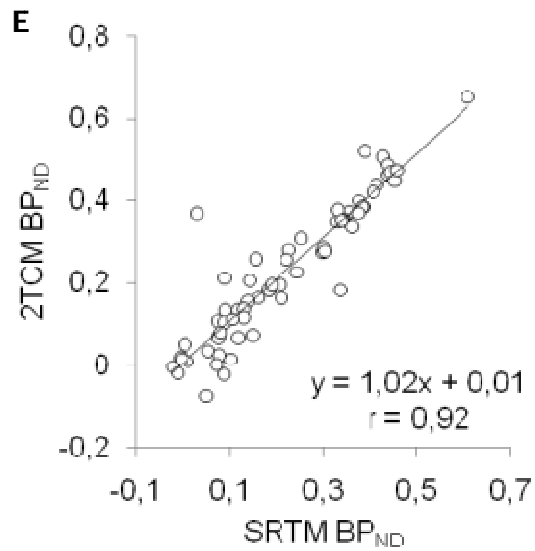
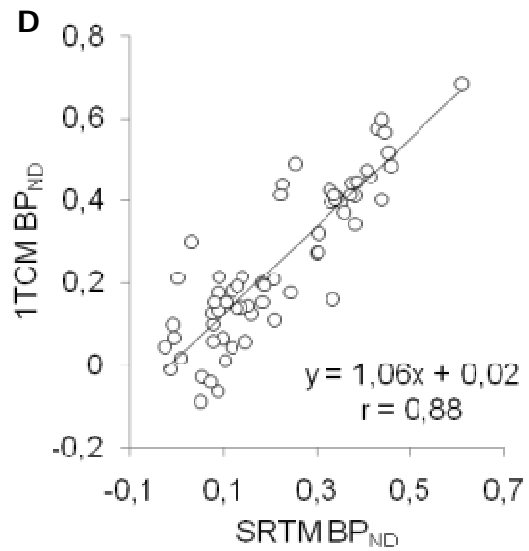
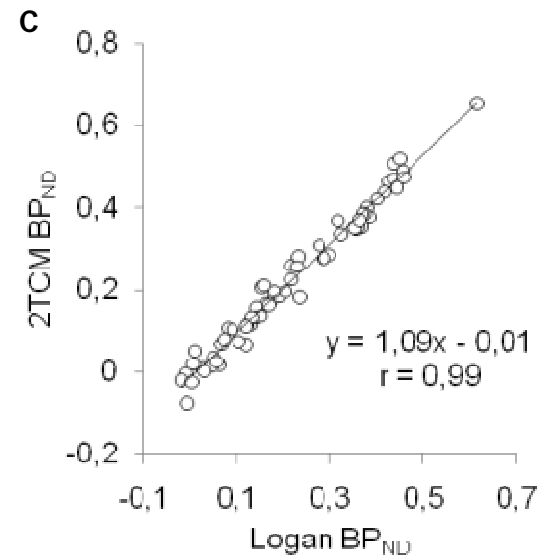
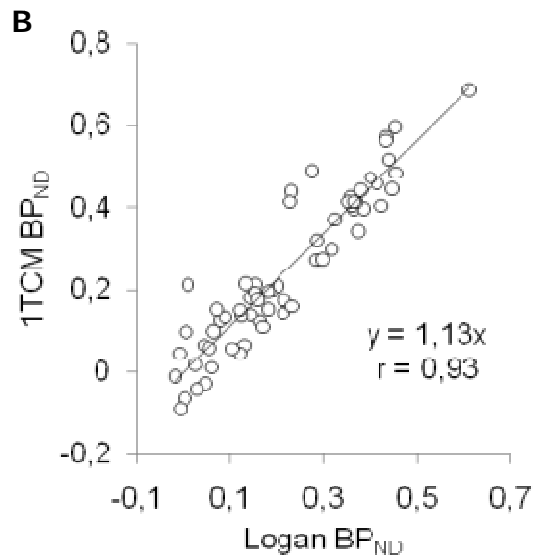
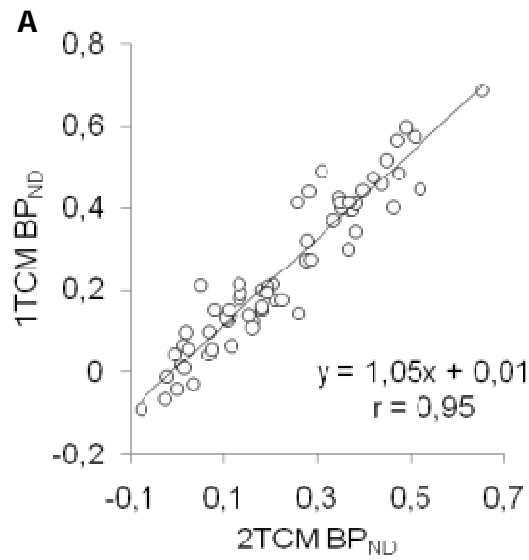
2TCM fits had lower Akaike's information criterion (AIC) value than 1TCM fits in 57 out of 80 (71%) cases. SRTM fits had lower AIC value than 2TCM fits in 69 out of 80 (86%) cases.



**Supplemental Figure 4.** Correlation of region-of-interest total distribution volumes ( $V_T$ ) of  $^{18}\text{F}$ -AMC20 obtained by Logan analysis with  $V_T$  values obtained by analyses with 1TCM and 2TCM models.

Points represent fits for individual regions in individual animals (both control and raclopride-pre-treated). Data for striatum, hippocampus, thalamus, hypothalamus, cortex, brainstem, cerebellum, olfactory bulbs and pituitary are used.

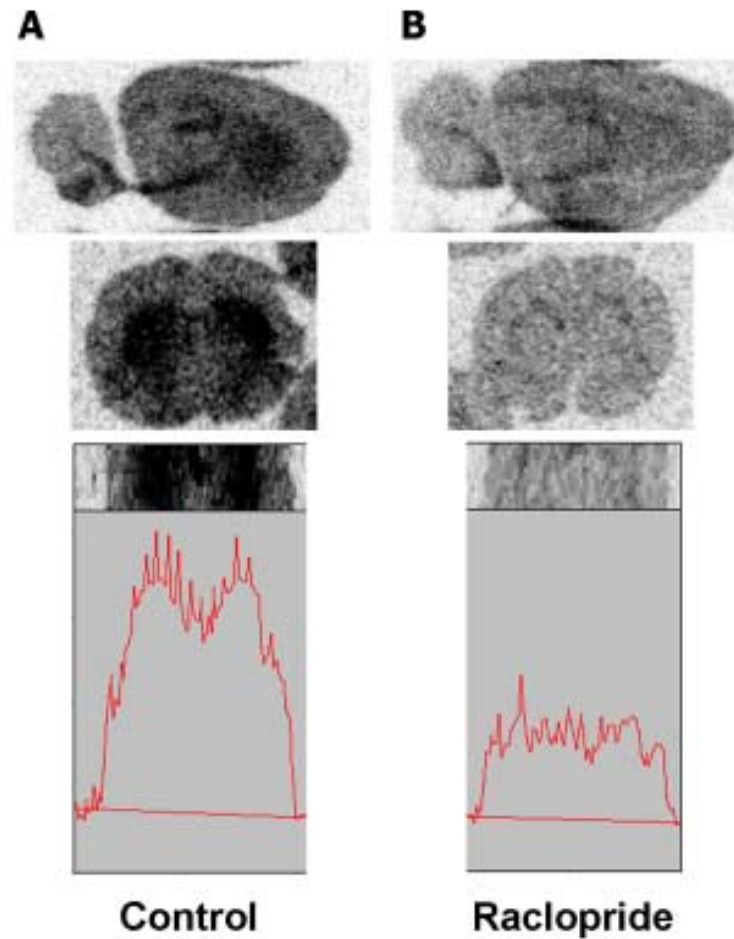
Unity line ( $x = y$ ) and linear regression lines for 1TCM and 2TCM data, along with their equations and r-criterion values are shown on the graphs.





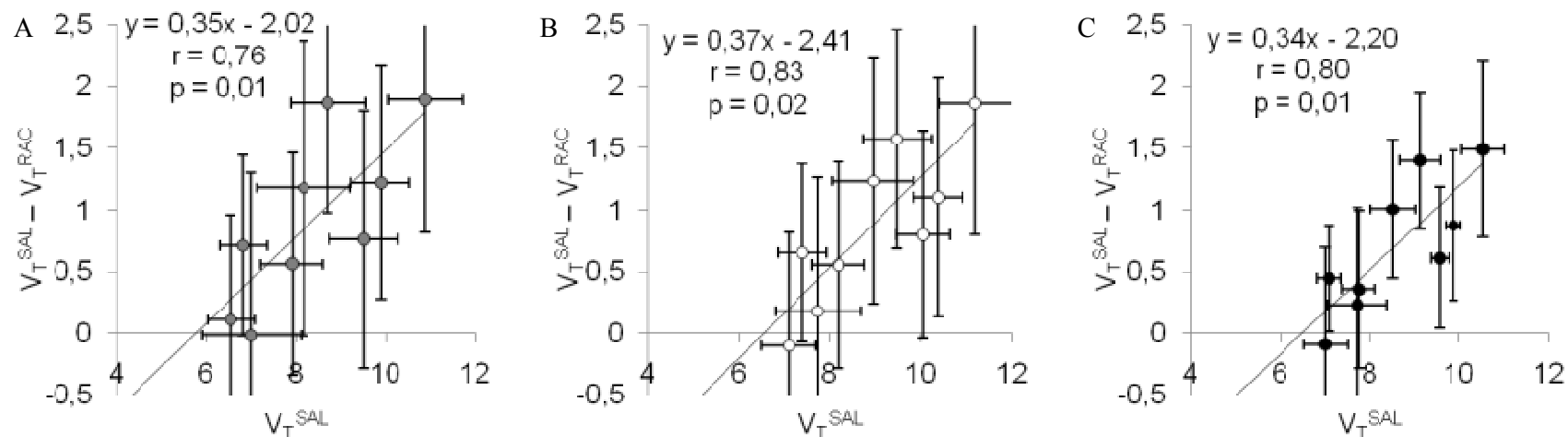
**Supplemental Figure 5.** Mutual correlation of region-of-interest binding potential ( $BP_{ND}$ ) values of  $^{18}F$ -**AMC20** obtained from different models. A – correlation of 1TCM and 2TCM  $BP_{ND}$  values. B,C – correlation of Logan  $BP_{ND}$  values with 1TCM, 2TCM values. D, E, F – correlation of SRTM  $BP_{ND}$  with 1TCM, 2TCM and Logan  $BP_{ND}$  values. Linear regression lines, along with their equations and r-criterion values are shown on the graphs.

Points represent fits for individual regions in individual animals, both saline and raclopride-pre-treated. Data for the striatum, hippocampus, thalamus, hypothalamus, cortex, brainstem, olfactory bulbs and pituitary are presented.  $BP_{ND}$  values are calculated using the cerebellum as a reference region, therefore the data for the cerebellum are not presented. 2TCM  $BP_{ND}$  values are calculated from  $V_T$  estimates, not from individual rate constants.



**Supplemental Figure 6.** Ex vivo autoradiography images of <sup>18</sup>F-AMC20 uptake in control (A) and raclopride-treated (B) rats.

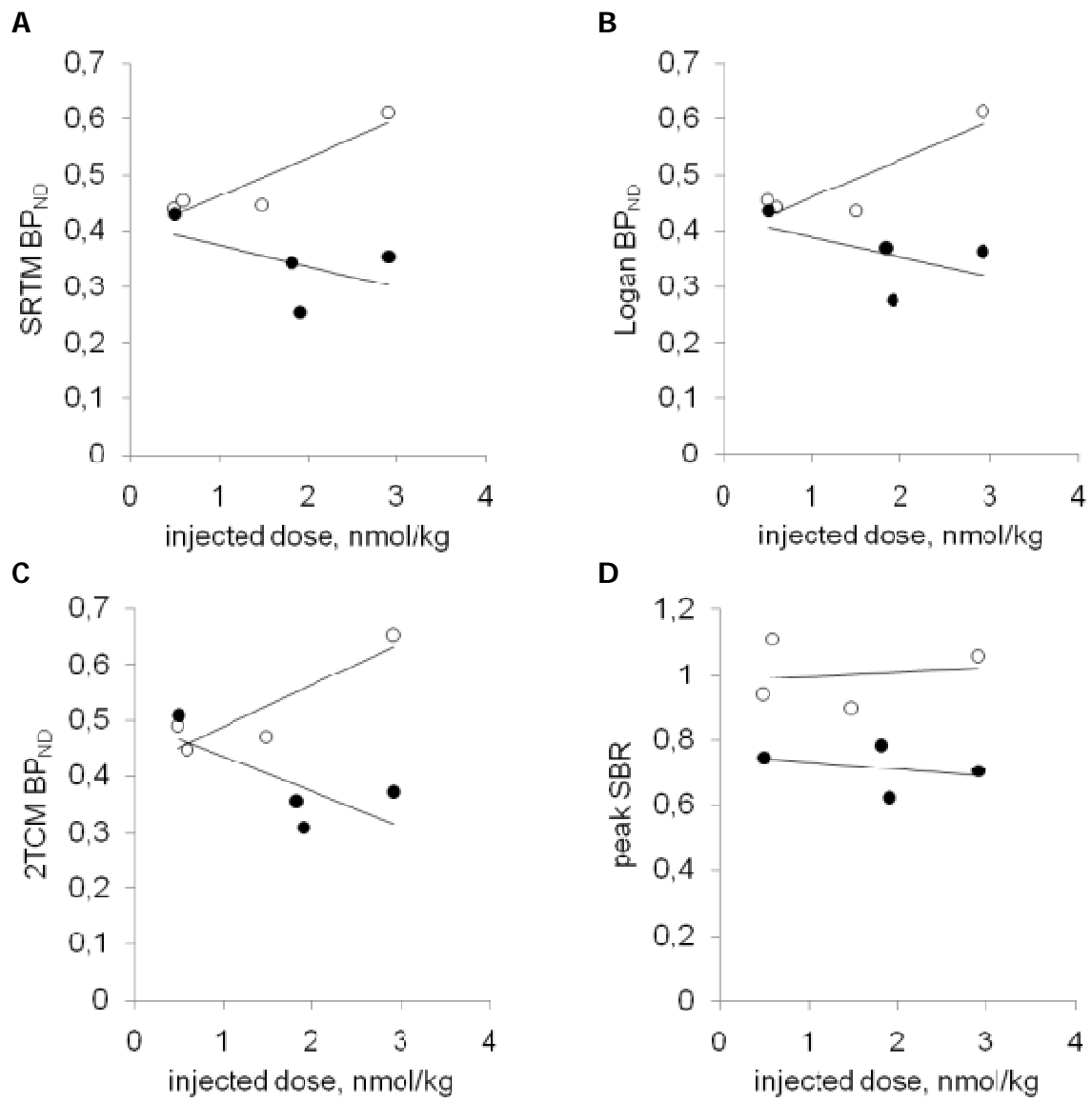
Representative sagittal and coronal slices are shown. Profile section through the striatum in coronal slices is presented at the bottom, showing absolute exposure values.



**Supplemental Figure 7.** Modified Lassen plots<sup>6</sup> built with  $V_T$  values from 1TCM (A), 2TCM (B) and Logan (C) analysis of  $^{18}\text{F}$ -AMC20 uptake.

Horizontal axes represent region-of-interest distribution volumes as baseline. Vertical axes represent the decrease of regional distribution volumes in raclopride-pre-treated rats relative to control rats. Assuming equal occupancy of receptors by raclopride and equal non-displaceable volume of distribution ( $V_{\text{ND}}$ ) of the tracer in all ROIs, the slope and the X-intersect of the linear regression line show, respectively, the fraction of receptors occupied by raclopride and the  $V_{\text{ND}}$ .

Data for striatum (always the rightmost topmost circle), hippocampus, thalamus, hypothalamus, cortex, brainstem, cerebellum (always the second circle from the left), pituitary and olfactory bulbs are used. Points represent means, error bars represent standard deviations. Equations of linear regression lines and r-criterion values are shown on the graphs.



**Supplemental Figure 8.** Relationship of injected doses of  $^{18}\text{F}$ -AMC20 with SRTM-derived (A), Logan-derived (B) and 2TCM-derived (C) striatal binding potentials (BP<sub>ND</sub>) and with PET-derived peak striatal specific binding ratios (D) in saline (open circles) and raclopride-pre-treated rats (closed circles).

Points represent measurements in individual animals. Linear trend lines are shown for each treatment group.

**Supplemental Table 1.** Ex vivo uptake (SUV units, mean±SD) of <sup>18</sup>F-AMC20 in brain and peripheral tissues of saline (SAL) and raclopride-pre-treated (RAC) rats.

Tissue	Saline (n=4)	Raclopride (n=4)
<b>Peripheral tissues</b>		
Adipose tissue	0.40±0.33	0.46±0.55
Adrenal glands	1.52±0.77	1.07±0.37
Bladder	2.37±1.90	1.04±0.61
Bone	0.09±0.03	0.12±0.02
Bone marrow	0.38±0.17	0.37±0.16
Caecum	0.20±0.07	0.26±0.07
Duodenum	2.74±2.99	1.14±0.45
Heart	0.15±0.06	0.12±0.03
Kidney	1.23±0.51	0.80±0.46
Large Intestine	0.45±0.42	0.36±0.19
LI Content	0.02±0.01	0.01±0.01
Liver	1.49±0.28	1.26±0.26
Lung	1.03±0.43	0.94±0.26
Muscle	0.19±0.10	0.17±0.04
Pancreas	1.41±0.56	1.24±0.49
Prostate	0.57±0.30	1.25±0.95
Small Intestine	0.18±0.09	3.25±3.63
SI content	0.41±0.48	25.8±28.6
Spleen	0.42±0.27	0.43±0.20
Stomach	1.60±0.77	0.81±0.41
Submandibular gland	0.74±0.33	0.68±0.21
Testes	0.44±0.14	0.48±0.08
Thymus	0.30±0.12	0.24±0.06
<b>Brain tissues</b>		
Cerebellum	0.16±0.07	0.13±0.03
Hippocampus	0.24±0.11	0.19±0.03
Medulla with pons	0.25±0.11	0.18±0.03
Midbrain	0.21±0.09	0.16±0.04
Olfactory bulbs	0.20±0.08	0.15±0.02
Pituitary	0.47±0.14	0.49±0.04
Rest of brain	0.23±0.10	0.18±0.04
Striatum	0.25±0.12	0.17±0.03
Thalamus + Hypothalamus	0.21±0.09	0.16±0.05
Total Brainstem	0.23±0.10	0.18±0.03
Total Cortex	0.20±0.09	0.17±0.04
Whole brain	0.21±0.09	0.17±0.04
<b>Bodily fluids</b>		
Whole Blood	0.21±0.06	0.14±0.06
Blood Cells	0.07±0.03	0.05±0.03
Plasma	0.34±0.10	0.20±0.08
Urine	20.0±15.3	17.1±10.6

**Supplemental Table 2.** 1TCM and 2TCM rate constant estimates of <sup>18</sup>F-AMC20 uptake in brain regions of control rats.

ROI	Rat	1TCM			2TCM				
		K <sub>1</sub> (ml/g/min)	k <sub>2</sub> (1/min)	AIC	K <sub>1</sub> (ml/g/min)	k <sub>2</sub> (1/min)	k <sub>3</sub> (1/min)	k <sub>4</sub> (1/min)	AIC
Striatum	A	1.03±0.04	0.09±0.01	465	1.70±0.94	2.13±4.73	2.57±3.17	0.19±0.12	461
	B	1.10±0.03	0.11±0.01	470	303±37758	1769±222120	5.93±3.00	0.10±0.04	447
	C	1.18±0.07	0.11±0.01	506	400*	1284*	3.32*	0.09*	483
	D	1.05±0.04	0.09±0.01	455	1.40±0.42	0.89±1.79	1.74±2.80	0.27±0.14	454
Hippocampus	A	1.00±0.05	0.10±0.01	475	2.07±0.72	2.44±2.39	1.64±0.89	0.14±0.03	459
	B	1.22±0.05	0.14±0.01	487	2.46±0.44	2.38±1.19	1.49±0.45	0.18±0.02	451
	C	1.21±0.08	0.14±0.02	506	1022*	2917*	2.86*	0.11*	470
	D	0.94±0.03	0.09±0.01	449	1.16±0.20	0.48±1.57	0.95±5.61	0.29±6.14	448
Thalamus	A	1.35±0.05	0.13±0.01	471	3.29±3.00	6.15±13.10	3.57±2.90	0.18±0.09	461
	B	1.40±0.06	0.15±0.01	487	3.45±1.88	5.08±0.58	2.65±4.27	0.20±11.77	468
	C	1.51±0.09	0.16±0.02	508	288*	872*	3.93*	0.13*	489
	D	1.25±0.05	0.12±0.01	459	1.36±0.14	0.22±0.18	0.22±0.61	0.32±0.36	461
Hypothalamus	A	1.20±0.05	0.13±0.01	469	1.70±0.25	0.83±0.70	0.92±2.03	0.25±2.56	457
	B	1.17±0.08	0.17±0.02	500	2.59±0.61	2.36±1.35	1.03±0.40	0.17±0.02	475
	C	1.09±0.07	0.14±0.02	504	22.7±121.3	67.7±396.6	2.79±1.06	0.12±0.03	482
	D	1.00±0.08	0.11±0.02	487	5.45±3.62	9.46±4.86	1.56±3.30	0.10±11.01	457
Cortex	A	0.75±0.02	0.09±0.01	444	0.75±0.03	0.09±0.01	1.33×10 <sup>-12</sup> ±0.01	0.09±958.27	448
	B	0.99±0.04	0.14±0.01	471	2.08±0.18	2.79±0.64	1.72±0.22	0.19±0.01	399
	C	1.09±0.05	0.13±0.01	485	498*	2332*	4.51*	0.11*	452
	D	0.71±0.02	0.09±0.01	431	182±25437	1739±245250	6.40±3.91	0.09±0.04	413
Brainstem	A	1.47±0.06	0.15±0.01	475	2.22±0.26	1.08±0.51	0.98±0.44	0.24±0.03	450
	B	1.31±0.06	0.16±0.01	487	2.53±0.30	2.14±0.73	1.31±0.30	0.21±0.02	441
	C	1.25±0.08	0.16±0.02	503	4.85±1.46	7.83±1.43	1.97±0.48	0.15±5.40	449
	D	1.21±0.05	0.13±0.01	456	1.79±0.16	0.95±0.39	0.94±1.12	0.22±1.48	428
Cerebellum	A	1.30±0.05	0.17±0.01	462	2.05±0.34	1.52±0.75	1.45±2.35	0.29±3.28	441
	B	1.30±0.05	0.21±0.02	478	2.40±0.31	2.27±0.87	1.47±0.40	0.27±0.02	435
	C	1.42±0.09	0.21±0.03	503	461.76*	1282*	3.13*	0.16*	454
	D	1.03±0.03	0.15±0.01	438	204±23305	1568±178070	7.31±177210	0.14±181530	419

(continued on the next page)

**Supplemental Table 2** (continuation). 1TCM and 2TCM rate constant estimates of  $^{18}\text{F}$ -AMC20 uptake in brain regions of control rats.

ROI	Rat	1TCM			2TCM				
		$K_1$ (ml/g/min)	$k_2$ (1/min)	AIC	$K_1$ (ml/g/min)	$k_2$ (1/min)	$k_3$ (1/min)	$k_4$ (1/min)	AIC
Olfactory bulbs	A	0.86±0.03	0.11±0.01	452	398*	2671*	5.30*	0.10*	433
	B	0.89±0.05	0.14±0.01	482	1.73±0.20	1.63±0.55	0.91±0.24	0.16±0.01	443
	C	0.93±0.05	0.13±0.01	483	2.84±1.11	6.08±0.89	2.27±1.40	0.15±7.44	449
	D	0.74±0.04	0.11±0.01	451	1.39±0.23	1.72±0.88	1.14±0.42	0.15±0.02	424
Pituitary	A	0.86±0.05	0.11±0.01	472	1.56±0.25	1.32±0.69	0.89±0.37	0.14±0.02	449
	B	0.94±0.06	0.16±0.02	491	1.93±0.42	1.96±1.12	0.95±0.40	0.16±0.02	468
	C	0.99±0.07	0.16±0.02	500	362±21029	1178±68329	2.55±68174	0.12±68981	467
	D	0.74±0.03	0.09±0.01	443	0.82±0.07	0.17±0.09	0.13±0.21	0.16±0.13	443

Data are presented as means±SD.

\* Standard deviation could not be estimated

**Supplemental Table 3.** Region-of-interest  $V_T$  measurements of  $^{18}\text{F}$ -AMC20.

Region of interest	Logan $V_T$		1TCM $V_T$		2TCM $V_T$	
	control	raclopride	control	raclopride	control	Raclopride
Striatum	10.53±0.48 (5)	9.04±0.53 (6)	10.89±0.83 (8)	8.99±0.69 (8)	11.21±0.80 (7)	9.34±0.70 (7)
Hippocampus	9.55±0.20 (2)	8.94±0.53 (6)	9.52±0.77 (8)	8.75±0.70 (8)	10.05±0.58 (6)	9.25±0.61 (7)
Thalamus	9.87±0.17 (2)	8.99±0.58 (6)	9.90±0.65 (7)	8.67±0.68 (8)	10.38±0.55 (5)	9.28±0.79 (9)
Hypothalamus	8.52±0.49 (6)	7.51±0.27 (4)	8.18±1.02 (13)	7.00±0.61 (9)	8.94±0.89 (10)	7.71±0.45 (6)
Cortex	7.76±0.37 (5)	7.40±0.52 (7)	7.92±0.69 (9)	7.36±0.58 (8)	8.19±0.56 (7)	7.63±0.62 (8)
Brainstem	9.11±0.44 (5)	7.72±0.34 (4)	8.72±0.82 (9)	6.85±0.34 (5)	9.48±0.76 (8)	7.91±0.45 (6)
Cerebellum	7.09±0.26 (4)	6.64±0.35 (5)	6.84±0.53 (8)	6.13±0.50 (8)	7.40±0.53 (7)	6.74±0.48 (7)
Olfactory Bulbs	7.01±0.48 (7)	7.10±0.63 (9)	6.56±0.52 (8)	6.45±0.67 (10)	7.09±0.61 (9)	7.18±0.69 (10)
Pituitary	7.72±0.67 (9)	7.49±0.42 (6)	7.02±1.10 (16)	7.03±0.72 (10)	7.74±0.94 (12)	7.55±0.55 (7)

Data are presented as means±SD ( $n=4$  per treatment group). Coefficients of variation (in %) are shown in parentheses.



**Supplemental Table 4.** BP<sub>ND</sub> of <sup>18</sup>F-AMC20 per brain region in control and raclopride-treated rats.

Region of interest	1TCM BP <sub>ND</sub>		2TCM BP <sub>ND</sub>		Logan BP <sub>ND</sub>		SRTM BP <sub>ND</sub>	
	Control	raclopride	control	raclopride	control	raclopride	control	raclopride
Striatum	0.59±0.07	0.47±0.08 (-21%) <sup>†</sup>	0.52±0.09	0.39±0.09 (-25%)	0.49±0.09	0.36±0.07 (-26%) <sup>†</sup>	0.49±0.08	0.35±0.07 (-29%) *
Hippocampus	0.39±0.06	0.43±0.02 (+9%)	0.36±0.07	0.37±0.08 (+4%)	0.35±0.06	0.35±0.08 (0%)	0.37±0.05	0.34±0.09 (-6%)
Thalamus	0.45±0.04	0.42±0.02 (-7%)	0.40±0.06	0.38±0.11 (-7%)	0.39±0.05	0.36±0.09 (-10%)	0.39±0.05	0.32±0.07 (-19%)
Hypothalamus	0.19±0.08	0.14±0.03 (-26%)	0.21±0.11	0.14±0.06 (-31%)	0.20±0.08	0.13±0.05 (-35%)	0.14±0.09	0.12±0.05 (-14%)
Cortex	0.16±0.04	0.20±0.02 (+27%)	0.11±0.02	0.13±0.06 (24%)	0.09±0.03	0.11±0.07 (22%)	0.08±0.01	0.10±0.06 (+18%)
Brainstem	0.27±0.06	0.12±0.04 (-56%) **	0.28±0.08	0.17±0.06 (-38%)	0.29±0.08	0.16±0.04 (-43%) *	0.29±0.08	0.14±0.03 (-53%) *
Olfactory Bulbs	0.03±0.06	0.05±0.09 (+97%)	0.02±0.04	0.07±0.11 (215%)	0.06±0.05	0.07±0.10 (25%)	0.07±0.05	0.07±0.12 (+2%)
Pituitary	0.02±0.11	0.07±0.09 (+227%)	0.05±0.11	0.05±0.10 (15%)	0.09±0.11	0.06±0.09 (-36%)	0.15±0.13	0.07±0.10 (-55%)

Data are presented as means±SD (n=4 per treatment group). Next to the BP<sub>ND</sub> values of the raclopride-treated group, percentage of change relative to the control group is shown. <sup>†</sup> P < 0.07, \* P < 0.05, \*\* P < 0.01, 2-sided Welch test

**Supplemental Table 5.** Comparison of  $^{18}\text{F}$ -AMC20 and  $^{18}\text{F}$ -FET-AMC13.

Parameter	$^{18}\text{F}$ -AMC20		$^{18}\text{F}$ -FET-AMC13*	
	mean baseline value	decrease after raclopride blockade <sup>†</sup>	mean baseline value	decrease after raclopride blockade <sup>†</sup>
In vitro striatal SBR <sup>‡</sup>	5.27±1.49	83%	3.56±0.86	72%
Peak striatal SBR (PET)	0.97±0.13	35%	1.08±0.25	17%
Striatal SBR (ex vivo autoradiography) <sup>§</sup>	1.48±0.34	41%	1.81±0.29	39%
PET striatal BP <sub>ND</sub> (by model) <sup>  </sup>	1TCM: 0.59±0.07	21%	0.63±0.08	25%
	2TCM: 0.52±0.09	25%	0.56±0.05	23%
	Logan: 0.49±0.09	26%	0.52±0.02	23%
	SRTM 0.49±0.08	29%	0.51±0.02	26%
V <sub>T</sub> -based striatal D <sub>2/3</sub> R occupancy by raclopride (by model) <sup>¶</sup>	1TCM:	35%		20%
	2TCM:	37%		25%
	Logan:	34%		21%
Average baseline PET SUV of the whole brain: maximum/end-of-scan	3.38±0.18/0.18±0.04		1.94±0.26/0.22±0.02	

\* data from our abstracts<sup>7</sup> and (Vladimir Shalgunov, unpublished data, 2014)

<sup>†</sup> 1 mg/kg approximately 30 min before tracer injection

<sup>‡</sup> radioligand concentration – 1.7 nM

<sup>§</sup> 35 min post-injection

<sup>||</sup> cerebellum as reference region

<sup>¶</sup> estimated from the modified Lassen plot

## LITERATURE CITED

1. Innis RB, Cunningham VJ, Delforge J, et al. Consensus nomenclature for in vivo imaging of reversibly binding radioligands. *J Cereb Blood Flow Metab.* 2007;27:1533–1539.
2. Van Wieringen J-P, Shalgunov V, Janssen HM, et al. Synthesis and characterization of a novel series of agonist compounds as potential radiopharmaceuticals for imaging dopamine D<sub>2/3</sub> receptors in their high-affinity state. *J Med Chem.* 2014;57:391–410.
3. Walenzyk T, Carola C, Buchholz H, König B. Chromone derivatives which bind to human hair. *Tetrahedron.* 2005;61:7366–7377.
4. Cohen N, Weber G, Banner BL, et al. 3,4-dihydro-2H-1-benzopyran-2-carboxylic acids and related-compounds as leukotriene antagonists. *J Med Chem.* 1989;32:1842–1860.
5. Kalaritis P, Regenye RW, Partridge JJ, Coffen DL. Kinetic resolution of 2-substituted esters catalyzed by a lipase ex *Pseudomonas fluorescens*. *J Org Chem.* 1990;55:812–815.
6. Cunningham VJ, Rabiner EA, Slifstein M, Laruelle M, Gunn RN. Measuring drug occupancy in the absence of a reference region: the Lassen plot re-visited. *J Cereb Blood Flow & Metab.* 2009;30:46–50.
7. Shalgunov V, van Wieringen J, Sijbesma J, et al. Evaluation of <sup>18</sup>F-AMC-15, <sup>18</sup>F-FPr-AMC-13 and <sup>18</sup>F-FEt-AMC-13 as candidate dopamine D<sub>2/3</sub>-agonist radioligands for PET [Abstract]. *J Nucl Med.* 2013;54:1108.